Pergamon

Cement and Concrete Research, Vol. 26, No. 7, pp. 1095-1107, 1996

0008-8846/96 $15.00 + .00

PII S0008-8846(96)00076-2

CARBONATION AND ELECTROCHEMICAL CHLORIDE EXTRACTION FROM CONCRETE

N.M. Ihekwaba*, B.B. Hope* and C.M. Hansson†
*Civil Engineering Dept.; †Materials & Metallurgical Eng. Dept.
Queen's University, Kingston. Ontario, Canada. K7L 3N6

(Refereed)
(Received December 4, 1995; in final form April 16, 1996)

ABSTRACT

Chloride ingress into steel reinforced concrete (r.c.), and the subsequent application of electrochemical chloride extraction (ECE) are shown to be considerably retarded by the presence of a carbonation front. Four concrete blocks each reinforced with two layers of steel mats in two different configurations were electrochemically treated. One block of each type was initially carbonated to a depth of about 30 mm, and subsequently ponded with saturated chloride solution (as NaCl) for 18 months. Electrochemical treatment using an applied current density of 1 A/m^2 of concrete surface was applied after sampling the concrete's chloride ion profiles. Carbonated concrete specimens operated at about twice as much polarizing voltage at the same applied current density as the non-carbonated concrete specimens. Higher chloride extraction was obtained in non-carbonated concrete than in carbonated concrete blocks irrespective of the configuration of the reinforcement system. Accumulations of alkali ions were greater in the non-carbonated concrete specimens in addition to higher initial chloride ion concentrations, and this was significantly greater in the specimens reinforced with different rebar mats at the top and lower sections. The changes in alkali ion accumulations followed a similar trend as chloride ion profiles. Hence, any softening effect due to these alkalies on the cement silicate hydrates is expected to be more pronounced in the non-carbonated than carbonated concrete. It is predicted that chloride contaminated concrete which has its cover considerably carbonated will likely show an inefficient ECE performance.

Introduction

Many environmental phenomena are known to significantly influence the durability of cement-based structures [1-6]. In steel reinforced concrete, the protection offered by the highly alkaline pore solution (pH > 12.5) can be destroyed by ingress of chloride (Cl^-) ions or by loss of alkalinity due to carbonation. The damage is largely dependent on the concrete properties and environmental factors. In urban and industrial areas, where environmental pollution results in

a significant concentration of CO_2, carbonation-initiated reinforcement corrosion can be the cause of concrete deterioration. However, Cl^- ions are the principal cause of steel reinforcement corrosion when deicing salts come in contact with reinforced concrete, or in marine or coastal environments. This is also the case where concreting practice includes contaminated ingredients or Cl^- ions are intentionally added. The effect of carbonation in lowering the pH of concrete can also be an incentive for Cl^- ions to cause severe corrosion damage to steel reinforced concrete.

The carbonation process starts with the diffusion of CO_2 into the concrete and its dissolution in the pore water [1,4,6] to form a weak acid. The acid subsequently dissociates into carbonate and hydrogen ions [1,4], and reacts with the hydroxide compounds to form the less soluble carbonates. The different stages of the carbonation process are briefly explained in the form of Equation 1. Since the solubility of calcium carbonate in the pore solution is limited, it tends to precipitate in the pore structure.

$$\begin{aligned} H_2O + CO_2 &\rightleftharpoons 2H^+ + CO_3^{2-} \\ H_2O + CO_2 &\rightleftharpoons HCO_3^- + H^+ \\ HCO_3^- &\rightleftharpoons CO_3^{2-} + H^+ \\ Ca(OH)_2 + 2H^+ + CO_3^{2-} &\rightarrow CaCO_3 + 2H_2O \end{aligned} \qquad (1)$$

The precipitation of the carbonates in the cement pores results in a decrease in concrete permeability and an increase in the electrical resistivity as well as the neutralization of the pore solution. As the carbonation process continues well after the cement pore solution is neutralized, the solid phases of the cement paste also react with the dissolved CO_2 producing in the final state an amorphous $CaCO_3$, $CaSO_4$, $Al(OH)_3$, SiO_2, and H_2O [1,3,6]. The extent of the carbonation front, which is a narrow zone with different pH and micropore composition on each side, depends on many variables including w/c ratio, cement type and proportion, as well as the concrete's moisture content and resistivity. It is reported that similar reactions of the other alkali hydroxides of sodium and potassium also play some role in the carbonation process [1,3]. Since the carbonation reaction results in decreased permeability and increased resistivity, carbonated concrete is likely to experience significantly higher resistance to ionic migration during the application of electrochemical chloride extraction (ECE).

The basic features of ECE are well documented in literature [7 - 12], and the process is based on similar electrochemical principles to those of impressed current cathodic protection (CP). The distinguishing features include the greater long-term costs and logistics required to operate and maintain CP compared with ECE systems, and the significantly higher applied cathodic current densities necessary to drive ECE systems. An inert anode material is used in order to inhibit electrochemical material dissolution in an alkaline electrolyte. Since both the ionic reaction products associated with the ECE process and those ions in the pore solution are mobile, they can migrate to the electrode of opposite polarity in accordance with the Nernst-Planck mass transport law (11-13). Some other contributory processes such as diffusion and convection are usually negligible. The supporting electrolyte penetrates into the concrete by direct absorption and electro-osmotic permeation. Negatively charged ions (particularly the chlorides) are thus extracted as they migrate towards the external anode. At the same time, the alkali metal ions accumulate in the region of the rebars where they react with the OH^- ions produced by the cathodic reactions.

TABLE 1
Concrete Mix

OPC, Type 10	370 kg/m^3
Sand	740 kg/m^3
Stones, 10 mm max	934 kg/m^3
Water	185 kg/m^3
AEA	6 %

Experimental Procedure

Four reinforced concrete blocks measuring 0.50 m × 0.50 m × 0.30 m high were cast using a concrete with w/c ratio of 0.5, and the mix proportion is shown in Table 1. Each block was reinforced with a steel mat system fabricated from 20M (ASTM #6) deformed rebars. Two blocks, denoted as #1 and #3, were reinforced with rebar mats in which the top and lower mats had their individual rebars aligned over each other as shown in Figure 1. The remaining two blocks, referred to as #2 and #4, had similar top mats as in #1 and #3 but with the lower mat configured such that the rebars were displaced with respect to those of the top mat as shown in Figure 2. Concrete blocks #1 and #2 were initially carbonated by intermittent exposure to CO_2 in a sealed chamber for about six months. The changes in alkalinity associated with the carbonation process were observed by spraying an acid-base indicator (Phenolphthalein) solution on freshly drilled holes on the concrete [1]. Measurements indicated an average carbonation depth of about 30 mm of concrete cover. Subsequently, all four concrete blocks were ponded with saturated NaCl solution for eighteen months and the Cl^- ion profiles are described below.

The experimental set-up of the ECE tests to the reinforced concrete specimens is schematically shown in Figure 3. Each concrete block was fitted with a leak-proof trough at the top surface to hold 0.1 M sodium borate (Na_3BO_3) electrolyte solution. All anode systems were fabricated from inert titanium wire mesh (ELGARD EC300™), with an areal coverage based on the top surface of the block. The rebar mats were electrically coupled to the negative terminal of a DC power source incorporating a 1.5 Ω shunt for periodic monitoring of the applied current distribution, and the circuit completed by connecting the positive terminal to the external anode.

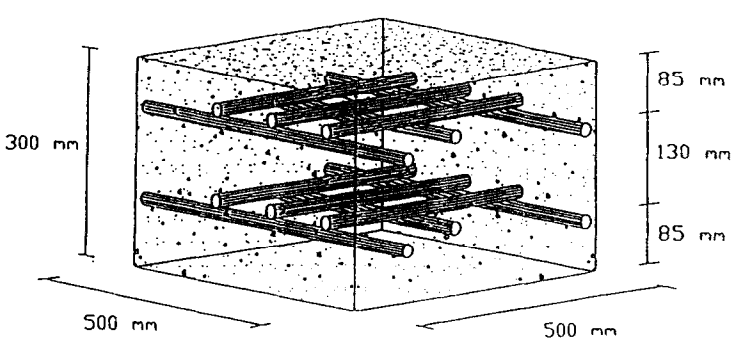

FIG. 1.
Schematic of ECE concrete blocks with aligned steel mat geometry (Specimens #1 & #3).

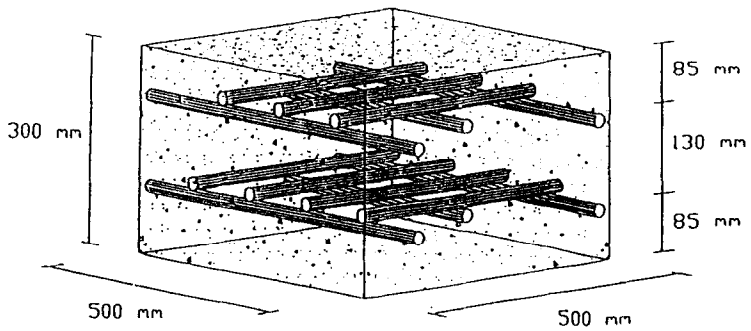

FIG. 2.
Schematic of ECE concrete blocks with displaced steel mat geometry (Specimens #2 & #4).

Electrochemical treatment of the concrete blocks was accomplished by cathodically polarizing the rebars using a direct current density of 1.0 A/m^2 of concrete surface in electrolytic contact with the anode system. This resulted in the transport of anions and cations due to the repulsive electrical potential of the rebars and external anode respectively. Anions such as the free chlorides (Cl^-), hydroxyls (OH^-), carbonates (CO_3^{2-}), and sulphates (SO_4^{2-}), are preferentially repelled from the vicinity of the rebars and migrate away from the cathode region in the direction of the anode. Similarly, cations such as calcium (Ca^{2+}), potassium (K^+), and sodium (Na^+) ions migrate towards the cathodic steel region. Migration of ions is basically related

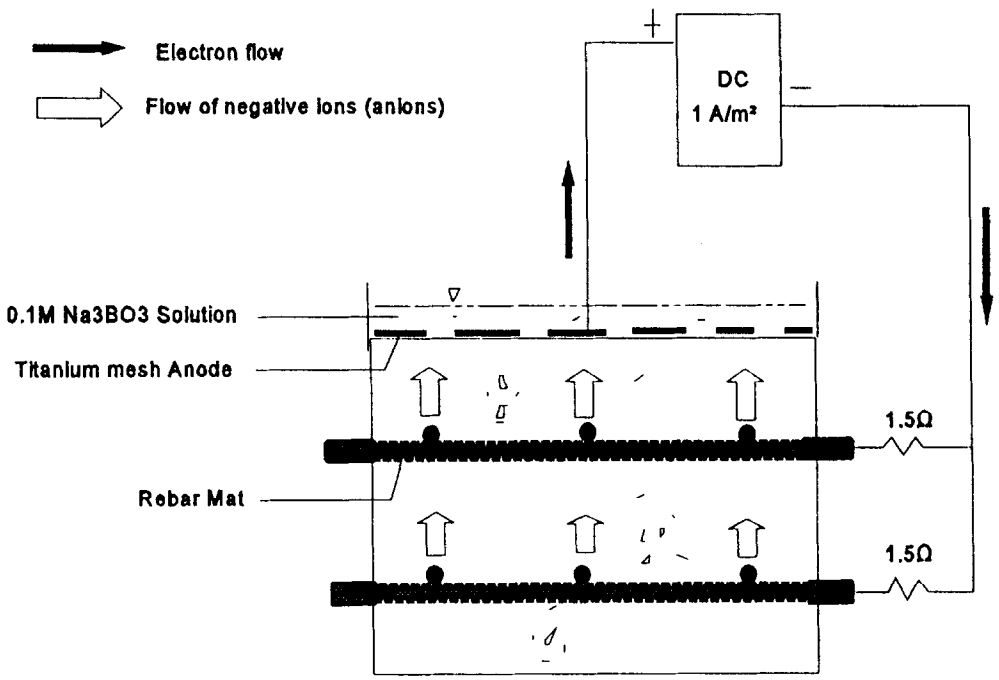

FIG. 3.
Schematic of electrochemical chloride extraction set-up.

to their transport (or transference) numbers, which is defined as the amount of total (applied) current carried by individual ions in relation to that carried by other ions during migration.

Concrete cores obtained before and after the ECE application, were sliced and pulverized for ionic analysis. Chloride ion determination was carried out by auto-titrating against 0.02M silver nitrate ($AgNO_3$) using a microprocessor ion analyser which was coupled with a solid-state chloride ion activity double-junction reference electrode and pH electrode. Total chlorides were analysed after digesting the concrete powder samples in concentrated nitric acid (HNO_3), while analysis of free chlorides were by digesting in water. Chemical analysis of sodium (Na^+) and potassium (K^+) ions was carried out by atomic absorption spectrophotometry using protocol outlined by Perkin Elmer for system 1106A [14].

Results

The initial potential mapping of the concrete test blocks indicated corrosion activity in specimens of both types especially at the top steel mats. Electrochemical corrosion potential of both steel mats and the macrocell current flowing between top and bottom mats before and after ECE application are shown in Table 2.

Chloride analysis of concrete cores before treatment indicated more chlorides within the cover of non-carbonated than the carbonated concrete specimens as expected. The Cl^- concentration profiles are shown in Figures 4 and 5. An average total (acid-soluble) chloride ion concentration of between 3500 - 8000 ppm (by concrete weight) was determined in the concrete cover of non-carbonated blocks #3 and #4 compared with a range of about 1500 - 3000 ppm (by concrete weight) in carbonated blocks #1 and #2. Also, the ionic analysis indicate that the Cl^- ion concentrations below the top mats of all four concrete blocks was insignificant.

The potential between the external anode and embedded rebars, as well as the applied current distribution to the top and lower rebar mats as monitored during the ECE application are shown in Table 3. It was observed that the polarizing voltage required for electro-migration was much higher for the carbonated blocks #1 and #2 than the non-carbonated blocks #3 and #4. The effect of the different Cl^- ion contamination levels as well as the increased concrete resistivity due to carbonation likely contributed to the different rates of ionic migration.

These results illustrate interesting features of chloride diffusion as a function of concrete carbonation. When chlorides ingress into carbonated concrete, the initial chloride concentration

TABLE 2

BLOCK	MACROCELL CURRENT mA		CORROSION POTENTIAL mV (vs CSE) *	
#	Pre-ECE	Post-ECE	Pre-ECE	Post-ECE
1	1.06	0.53	- 341 / - 180	-255 / - 148
2	1.03	0.33	- 376 / - 288	- 293 / - 247
3	1.68	0.67	- 293 / - 103	- 205 / - 48
4	1.75	0.67	- 290 / - 86	- 205 / - 50

profile is somewhat lower in concrete reinforced with uniformly configured steel mats, as in Figure 4a, than with displaced reinforcement geometries (Figure 5a). While for the non-carbonated blocks, the reverse is true as shown in Figures 4b and 5b respectively for the two steel mat types. Carbonation also affected the effectiveness of the ECE treatment. The total chloride ion concentration of the carbonated concrete specimen #1 (Figure 4a) was reduced from the initial level of about 2600 ppm (by concrete weight) to about 1800 ppm after treatment. The soluble chlorides were reduced by approximately the same amount. The corresponding non-

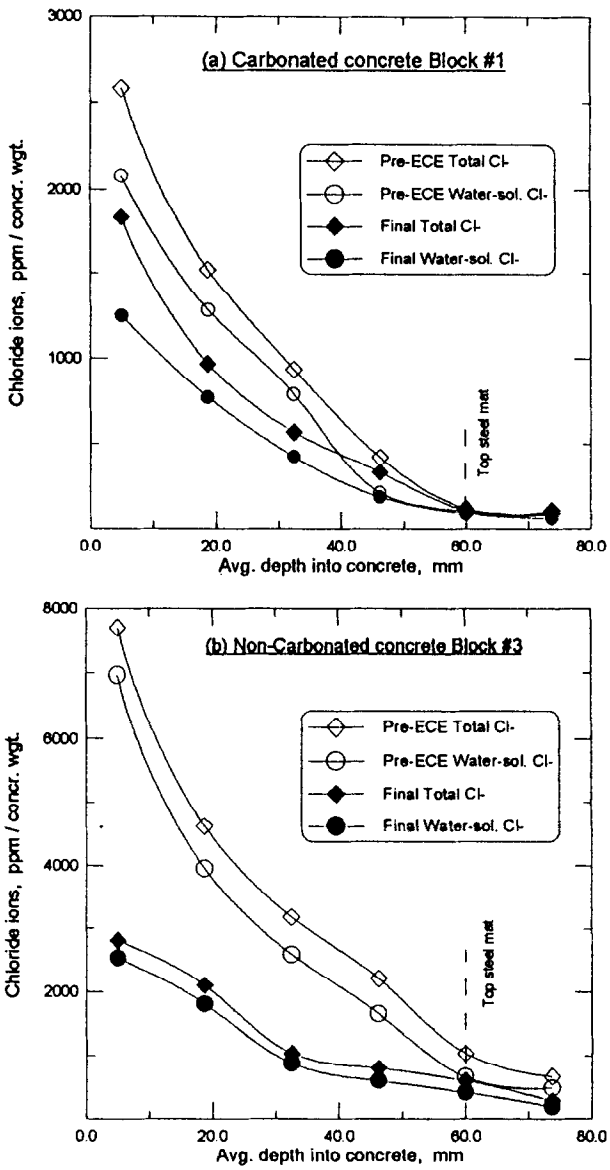

FIG. 4.
Chloride profiles in ECE systems with steel mats aligned.

carbonated specimen had a significantly higher initial Cl^- ion level (7800 ppm) but a much higher removal (~ 2900 ppm). Similar relative behaviour was observed for the specimen with displaced rebar mats (Figures 5a & 5b).

The influence of concrete carbonation on the redistribution of sodium (Na^+) and potassium (K^+) ions is shown in Figures 6 and 7, respectively. Contributions to the Na^+ profile will include sodium from the cement paste, from the NaCl, and from the sodium borate (Na_3BO_3) electrolyte

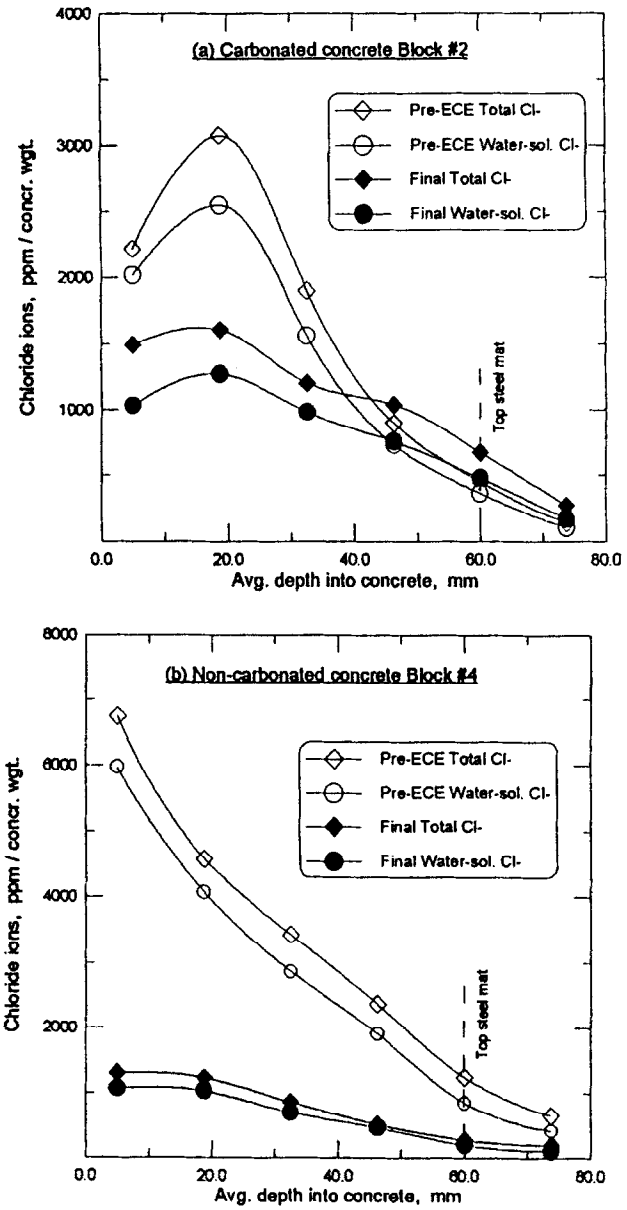

FIG. 5.
Chloride profiles in ECE systems with steel mats displaced.

whereas the only K^+ is that from the cement. In addition, the rebar geometry had a strong influence on the distribution of applied cathodic current density to the steel mats and hence on the accumulation of the cations. But it is only the Na^+ ions which were originally in greater concentration that appear to show greater accumulations especially in the non-carbonated concrete compared with the carbonated concrete samples. The potassium (K^+) ion profiles, however, showed a much higher increase in ionic concentration in sampled locations of carbonated block #1 than in non-carbonated block #3, although both had similar reinforcement systems. However, when the reinforcement system is changed as in block #2 (carbonated) and #4 (non-carbonated) as shown in Figure 7, the K^+ ion profiles indicated substantially higher increases in non-carbonated specimen #4 after ECE application than in carbonated specimen #2. In all ECE specimens, the initial K^+ ions were between 500 - 1500 ppm (by concrete weight), which increased to a range of 1200 - 3700 ppm (by concrete weight) after treatment. It is observed though, that the final K^+ ion content of block #4 was somewhat higher at the sampled points than in any other ECE specimen.

Discussion

The properties of cement-based systems, such as the test specimens, can be harmfully affected by the physico-chemical processes of carbonation which include the dissolution of the solid $Ca(OH)_2$ in the pore water, the reduction of the pore volume due to the solid products of hydration and carbonation as well as the condensation of the water vapour on the walls of concrete pores which may be in equilibrium with the ambient relative humidity and temperature [5]. However, these chemical changes, including the reduction of pH from about 13.5 to below 9.0, can retard chloride permeation and the chemical reactions associated with chloride ion binding by cement can be improved. Moreover, in some cases these carbonation reactions can cause an increase in concrete properties such as shrinkage, density and compressive strength as a result of fundamental changes of the pore structure [1]. The lower initial chloride ion profiles of blocks #1 and #2 compared with blocks #3 and #4 [1] can be attributed to these factors.

Despite a lower chloride ion content in the carbonated specimens, an increased electrical resistivity of the cement paste as a result of the carbonation process may require close attention for an efficient ECE application. The macrocell corrosion currents between the top and lower mats which indicate their different corrosion states, are lower for the carbonated blocks #1 and #2 although all steel mats of both systems are in non-carbonated concrete zones. However, the

TABLE 3

Block #	Rebar Mat Details	Concrete Cover	Potential between Anode and Steel Mats		Applied Current Distribution to Mats	
	Top/Lower	Before ECE	Start ECE	End ECE	Top	Lower
1	Uniform	Carbonated	23.5 V	12.9 V	85%	15%
2	Displaced	Carbonated	20.4	13.2	80	20
3	Uniform	Non-carbonated	12.2	8.4	90	10
4	Displaced	Non-carbonated	12.4	8.5	90	10

electrochemical corrosion potentials of the carbonated blocks were somewhat more negative than that of the non-carbonated blocks #3 & #4. Using Nernst law, it can easily be shown that the effect of the reduction in pH due to concrete carbonation will lead to higher electrochemical potential of the reinforcing steel embedded in the concrete. It has been demonstrated in a study [15] on steel corrosion in cement-based systems that carbonation has a strong influence on the electrochemical potential of steel rebars. It is also possible that a potential difference resulted from the proximity of the different concrete regions of different ionic composition in the top zone of the specimens since ions will not move at the same rate through them [16]. This means

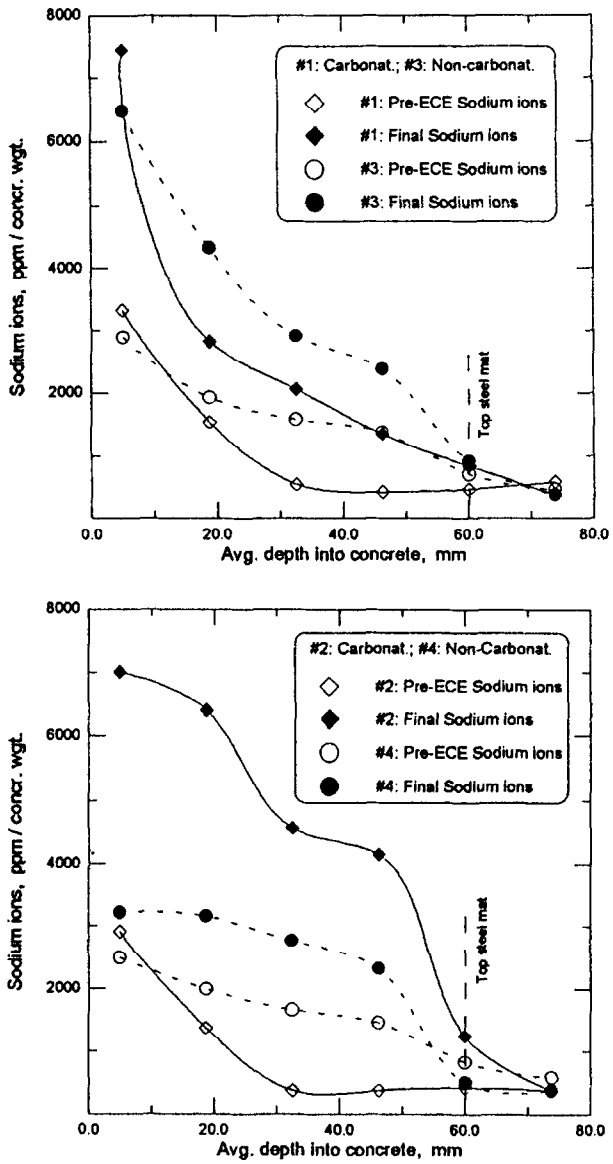

FIG. 6.
Profiles of sodium ions - (a) #1 & #3: aligned mats, (b) #2 & #4: displaced mats.

that the carbonated concrete zone (which is between the top mat and the external reference electrode used in the potential measurement), and the rest of the non-carbonated concrete becomes a source of a potential difference. Though ions of the higher concentration zone carry their charge into the other zones until a restraining field and potential exists, the differences will

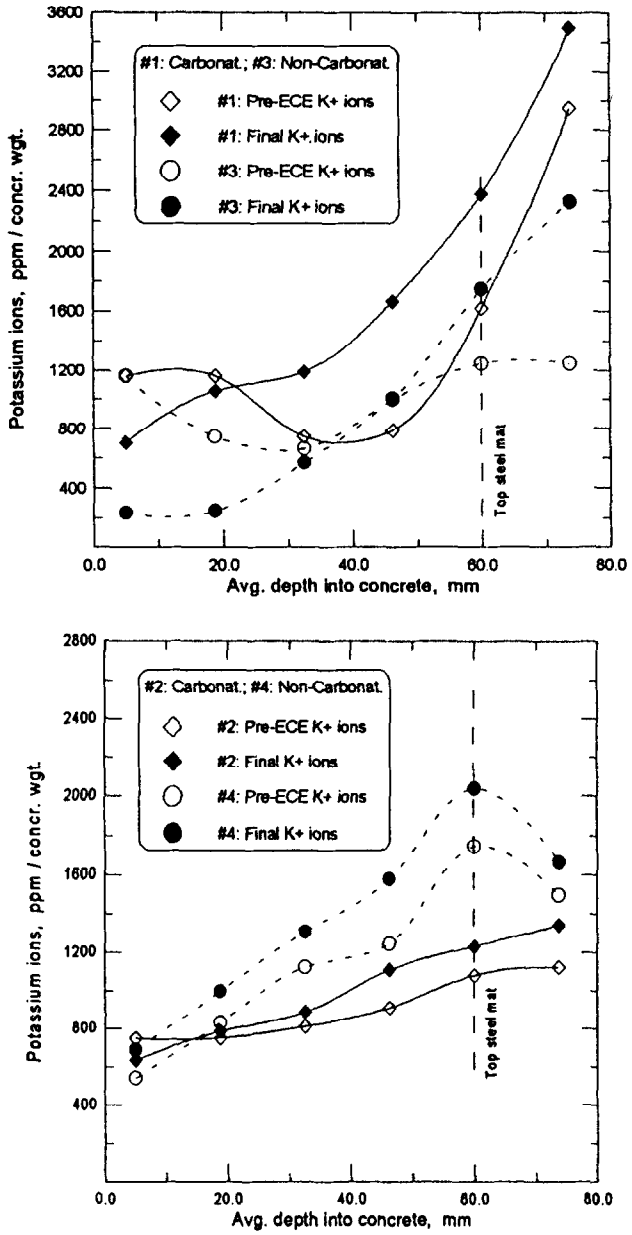

FIG. 7.
Profiles of potassium ions - (a) #1 & #3: aligned mats (b) #2 & #4: displaced mats.

persist as long as the source and receiver zones have different concentrations [16] which is more or less the case in carbonated specimens than in non-carbonated specimens.

As explained before, the direct consequence of the carbonation process in concrete is to significantly increase the concrete resistivity as the reaction products precipitate in the pore structure. This may be the case with specimens #1 and #2 in which the presence of the carbonation front may have caused relatively high total polarizing voltage initially at about 20.0 V, although decreasing to about 13.0 V at the end compared with a reduction from 12.0 V to 8.5 V for the non-carbonated specimens #3 and #4. Also, the variation in concrete resistivity may have influenced the applied current density distribution to the steel mats as well. The increased applied current flow to the lower rebar mats of these specimens compared with that of the non-carbonated specimens is most probably due to higher resistivities of the concrete cover.

The significantly greater reductions in ingressed chloride ion contents of non-carbonated concrete specimens (Figures 4b & 5b), irrespective of the steel reinforcement configuration, is also believed to be the combined effect of a more open pore structure and resultant lower concrete resistivity. It is known though that the more Cl^- ions that are extracted from the cement pores the lower the transport numbers [17], and hence the lower the extraction performance. Diminishing chloride migration with treatment time would then contribute to a decrease in system voltage usually observed in ECE systems with the consequent increase in applied current requiring constant control. In the later stages of extraction during an ECE application, it is also possible that there are fewer Cl^- ions to carry the electrical charge compared with the case at the onset of migration. In a similar investigation [10] incorporating admixed Cl^- ions in non-carbonated concrete and with both steel mats located within chloride contaminated concrete zones, a more efficient ECE performance was observed in systems reinforced with uniform steel mat geometries (at top and lower sections) than when the mats were displaced with respect to one another. This is not the case in this study because of such variables as the different Cl^- ion sources and their associated cations (which was a mixture of Na^+ and Ca^{2+} in the previous study), concrete hydration regimes and chloride contamination levels, capability of cement to bind Cl^- ions in its hydration products and their probable different transport numbers, as well as distribution of applied current density during ECE application. These parameters were clearly not similar in both cases of ECE application. Although both studies indicate the feasibility of extracting both admixed and ingressed chlorides in concrete systems reinforced with different configurations of steel mats, the amount of Cl^- ions trapped at the steel due to severe corrosion has not yet been ascertained and is currently under investigation.

When passive conditions are achieved as indicative of an efficient ECE performance, it is necessary from the point of electrochemical corrosion of rebars and concrete durability to check for any increase in cation accumulation in addition to a reduced residual Cl^- ion concentration in the cathode (rebar) region. It is recognised though that such unusual accumulation of the alkali cations may also cause damage to the cement paste phase. This can result from the formation of alkali hydroxides during electrochemical extraction provoking concrete softening by substantially increasing the solubility of the cement silicate hydrates [17,18]. In this study, it is difficult to base any prediction on changes in the Na^+ ion profiles because of the strong influence of the sodium-based electrolyte used in the tests. In fact the difference in Na^+ ion contents of all ECE specimens, irrespective of the form of reinforcement configuration is not clear. It is noted though that the presence of a carbonation front affected the ionic contents of specimens #1 and #2, such that these were more than twice the corresponding levels of the non-carbonated specimens #3 and #4 after ECE application (Figure 6), which may require further studies. On the other hand, redistribution of K^+ ions in all specimens showed a different trend.

When an ECE concrete specimen is reinforced with a uniform steel mat system, the residual K^+ ion profiles are more or less the same (with a variation of ~ 500 ppm) whether or not the concrete is carbonated (Figure 7a). In the case of non-carbonated concrete reinforced with differently configured steel mat systems, more K^+ ions accumulated towards the steel rebars after ECE application than when such concrete is carbonated (Figure 7b). The apparent dichotomy in results may well be the effect of the variation in form and composition of the carbonation reaction products in the micro pores, distribution in applied polarizing current densities to the rebars of each specimen, and inhomogeneities in concrete. It has been noted in previous studies that physical and chemical alteration of the cement paste in the cathode zone are possible, and that these were identified by their darker appearance [10] and more open micro-pores [19]. Moreover, the high concentration of these alkali metals coupled with the wetness associated with their electro-migration (which occur due to their small ionic radius) has been attributed to be responsible for observed bond loss in previous studies [20].

Summary

1. Chloride ion diffusion into hardened reinforced concrete is retarded by the presence of a carbonation front.
2. It is possible to extract chlorides from carbonated concrete but the process is less efficient than in non-carbonated concrete.
3. ECE concrete specimens reinforced with similarly configured steel mat systems show better chloride ion extraction than when the two layers have different geometries despite the presence of a carbonation front. In practice, rehabilitation of chloride-contaminated concrete structures may necessitate more than a single application of the ECE system depending on the form/geometry and placement depth of the reinforcing system.
4. Accumulation of 'total' alkali ions (Na + K) in the cathodic zones which includes the location of the rebars is substantially higher in carbonated concrete. Increases in the alkali concentrations are dependent on the applied current required for migration, reinforcement systems and geometry available for polarization, and the level of initial concrete chloride contamination.

Acknowledgment

Financial assistance was provided by the Natural Sciences and Engineering Research Council of Canada, as a strategic grant to Dr. C.M. Hansson and Dr. B.B. Hope.

References

1. M.G. Richardson, Carbonation of Reinforced Concrete: its Causes and Management, Citis Ltd, Dublin, pp. 205, 1988
2. J.N. Enevoldsen & C.M. Hansson, Cem. & Con. Res., v. 84, #7, pp. 1344-1352, 1995
3. R.L. Berger, J.F. Young & K. Leung, Acceleration of Hydration of Calcium Silicates by Carbon Dioxide Treatment, Nature Physical Science, v.240, #97, 1972, pp. 16-18
4. B. Jungermann, The Chemical Process of the Carbonation of Concrete, Betonwerk +Fertigteil-Technik, v.48, #6, 1982, pp. 358-362
5. V.G. Papadakis, C.G. Vayenas & M.N. Fardis, ACI Materials J., v. 88, #4, pp. 363 - 373, 1991

6. A. Rosenberg, C.M. Hansson & C. Andrade, Mechanisms of Corrosion of Steel in Concrete, Materials Science of Concrete, pp. 285 - 313, 1989
7. D.R. Lankard, J.E. Slatter, W.A. Holden & D.E. Niesz, Battelle Columbus laboratories Report DOT FHWA-RD-76-60, 1975
8. Ø. Vennesland, Proc. Nordisk Beton Kongress, Odense, Denmark, 1987
9. J.E. Bennett & T.J. Schue, paper #316, NACE Corrosion '90, Las Vegas, 1990
10. N.M. Ihekwaba, M.Sc. Thesis, Queen's University, Kingston, Ontario, 1992
11. C. Andrade, Cem. & Con. Res., v.23, #4, pp.724-742, 1993
12. C. Andrade, J. Diez, A. Alaman, & C. Alonso, Cem. & Con. Res., v.25, #4, pp.727-740, 1995
13. A.J. Bard & L.R. Faulkner, Electrochemical Methods: Fundamentals and Applications, John Wiley & Sons, 1980
14. Perkin Elmer, Atomic Absorption Spectrophotometry, System 1106A, 1988
15. J.A. Gonzalez, S. Algaba & C. Andrade, British Corrosion Journal, v.15, #3, pp.135-139, 1980
16. R.E. White, J.O'M Bockris, B.E. Conway & E. Yeager (ed.), 1984, Comprehensive Treatise of Electrochemistry, v.8, Experimental Methods in Electrochemistry, Plenum press, NY
17. B. Elsener, M. Molina & H. Böhni, Corrosion Science, v.35, #5-8, pp. 1563-1570, 1993
18. N.R. Buenfeld & J.P. Broomfield, Inter. conf. on Corrosion and Corrosion Protection of Steel in Concrete, Sheffield, U.K., pp. 1438-1451, 1994
19. P.F.G. Banfill, Inter. conf. on Corrosion and Corrosion Protection of Steel in Concrete, Sheffield, U.K., pp. 1489-1498, 1994
20. N.M. Ihekwaba, B.B. Hope & C.M. Hansson, paper submitted to Cem. & Con. Res., 1995